Indian Journal of Pure & Applied Physics
Vol. 64, February 2026, pp. 158-166
DOI: 10.56042/ijpap.v64i2.25358

Design and Analysis of Chiral MZI Based All-Optical Galois Field Adder

Arindam Changder[a,d], Kousik Mukherjee[b,c,*] & Jitendra Nath Roy[c,d]

[a]Department of Physics, Raniganj Girls' College, Raniganj 713 347, India
[b]Department of Physics, Banwarilal Bhalotia College, Asansol 713 307, India
[c]Center of Organic Spintronics and Optoelectronic Devices, Kazi Nazrul University, Asansol 713 340, India
[d]Department of Physics, Kazi Nazrul University, Asansol 713 340, India

Received: 7th November 2025; accepted: 31st December 2025

The design of a Chiral Mach-Zehnder interferometer based 4-bit all-optical Galois field adder operating at significantly low power. Quartz has been utilized as the chiral material which rotates the plane of polarization of a light signal and this polarization rotation is the backbone of the all-optical switching module. The presence or absence of the control signal significantly changes the output of the CMZI switch. This switching module solely gives the all-optical logic XOR operation and with the help of four such parallel XOR gates we can design a CMZI based 4-bit all-optical Galois field adder. The circuit has been analysed by calculating performance indicating parameters such as amplitude modulation (AM~0.008695 dB), extinction ratio (ER~13.27 dB), contrast ratio (CR~16.28 dB), Q-factor (Q~34.48 dB), relative eye opening (REO~ 95.29 %) etc to establish the practical feasibility of the device. These satisfactory values suggest that this device may play a significant role in advancing the next generation optical technologies.

Keywords: All-optical logic gates, Galois field, Chiral mach-zehnder interferometer (CMZI), Adder, Optical arithmetic operation

1 Introduction

In recent decades, it has been shown that optical signal processing has emerged out as an alternative approach over the electronic one because not only due to the limited speed but also for its innate parallelism. Over the last few decades, several schemes have been proposed to achieve all-optical computation at ultra-low power and also at ultra-high speed. Some notable designs have been already proposed to achieve all-optical logic and arithmetic operations where several optical components have been used like photonic crystal[1-2], semiconductor optical amplifier (SOA)[3-4], quantum-dot SOA[5-6], nonlinear optical loop mirror (NOLM)[7-8], terahertz-optical-asymmetric-demultiplexer (TOAD)[9-10], waveguides[11-12], ring resonators[13-14]etc.

Out of various arithmetic operations, addition is one of the most fundamental operations which are used in numerous times in building easy to harder blocks of a computing network.

Different half and full adders have been already designed in the all-optical domain for general-purpose arithmetic operations[15-17], but the Galois field adders are specialized components that are particularly designed for applications which require arithmetic operations in finite field.

In mathematics, a Galois field is a field that contains a finite number of elements. A GF (2^n) contains all n-bit combinations which can be shown in the form of different powers of 'p'; where, p is the primary element of the Galois field. Thus, GF (2^n) has 2^n elements which are 0, 1, p^1, p^2, p^3,.., p^{2n-2}. Each GF has an n-order primitive polynomial whose root is 'p'.

The unique mathematical properties of Galois fields, also known as the finite fields, are extensively utilized to achieve widespread applications[18].

Therefore, the Galois field adder plays a significant role in the field of optical and quantum computation in terms of arithmetic operation, high speed signal processing, error correction and cryptography[19].

In the realm of photonics & opto-electronics, chiral materials are extremely useful where, the advancement of all-optical circuit designs is concerned because of their unique light-matter interactions in comparison with the other optically active materials[20-22]. They can rotate the plane of polarization in a significant manner. Chiral materials have some salient properties which are very

*Corresponding author: E-mail: klmukherjee003@gmail.com

significant in all-optical computation like they are able to respond to the electric field vector of light signals even at the nano range, offer wavelength tunability governed by geometric manipulation, while allowing dynamic switching at ultra-fast speeds.

Additionally, they exhibit some more significant properties like reversible chiroptical switching with visible-light responsiveness[23]. The thermal stability of chiral material allows all-optical switching at room temperature and operates on the principle of light-matter interaction in them[24-25].

Chiral material-based Mach-Zehnder interferometer i.e., CMZI has some influential applications in the all-optical signal processing like, ultra-fast switching at ultra-low power along with higher band-width has already been achieved[26] and the values of different performance parameters such as amplitude modulation, extinction ratio, contrast ratio, Q-factor, relative eye opening etcare also found to be satisfactory. The data rate of this proposed switching module is ~ 100 Gbps[27-29].

Here, it is to be mentioned that the CMZI based Galois field adder has yet not been reported in the domain of optical computation. Especially, GF adders find application in pseudorandom binary sequence generation[30,31].

Hence, the design of an all-optical Galo is field adder using CMZI have been proposed and analysed with the help of numerical simulation using SCILAB.

2 Theory

2.1 Principle of Operation of CMZI and its Theoretical Modelling

A horizontally polarized (HL) probe signal and a vertically polarized (VL) control signal of equal intensities are combined at the first beam combiner (BS-01) and then the combined beam is separated equally in both the arms of the interferometric circuit. A chiral material (in this case, quartz) of length 7.5 mm is there at the upper arm and at the lower arm there exists a phase shifter in the CMZI. The quartz crystal provides 12° rotation/mmin the plane of polarization i.e., it converts a HL into VL and vice-versa.

Signals emerging out from both the arms then interfere at the second beam combiner (BS-02) and the signals coming out from BS-02 are received from the two arms as outputs of CMZI. Here, the final output emerged out from the Port-I, after passing through a horizontal polarizer serves the all-optical XOR logic operation[28]. The output beam from port-II is blocked with the help of a beam blocker, due to its performance lag[27]. Beam blocker is generally employed to selectively suppress the undesired signal arising in the realization of all-optical circuits is shown in Fig. 1.

It was numerically found that the values of amplitude modulation and quality factor at the port-II are 3.01 dB and 2.8001 respectively. Therefore, the port-II is not utilized due to the poor performance in the all-optical operation. The truth table for all-optical XOR logic operation is provided in Table 1.

The theoretical modelling of this fundamental switching element has been thoroughly discussed in our previous papers[27-29]. In the presence and absence of the control signal (CS), the output intensities of the Port-I of CMZI are given by,

$$I^1 = \frac{I_o}{2}\left[\eta_1 + \eta_2 - 2\sqrt{\eta_1\eta_2}\cos\left(\frac{2\pi\vartheta}{c}\Delta L\right)\right] \quad \ldots (1)$$

$$I^0 = \frac{I_o}{4}\eta_1 \quad \ldots (2)$$

where, I^1& $I^0$are the output intensities in the presence (CS=1) and absence (CS=0) of the control signal, I_0 being the total intensity of the input signal. $\eta_1 and\ \eta_2$ are the total effective transmittances at the upper and lower arm of the CMZI respectively. ΔL is the optical path difference (OPD), which is maintained by using a particular length of the chiral

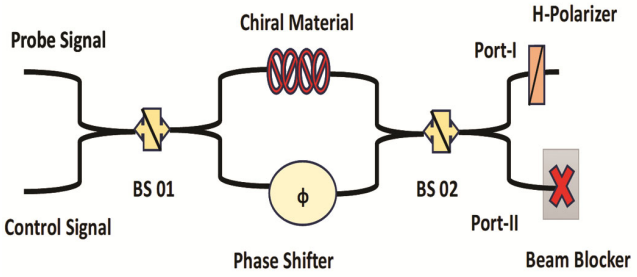

Fig. 1 — All-optical design for Chiral-MZI

Table 1 — Truth table of XOR

Input		Output
Probe Signal (PS)	Control Signal (CS)	Output at Port-I (PS XOR CS)
0 (NL)	0 (NL)	0 (NL)
0 (NL)	1 (VL)	1 (HL)
1 (HL)	0 (NL)	1 (HL)
1 (HL)	1 (VL)	0 (NL)

material (CM).The frequency of the input signals i.e., ϑ has been taken to be similar that of used by reference[26] and c is the speed of light in vacuum.

2.2 The proposed Design & Operational Behaviour of Galois Field Adder

All-optical circuit diagram for CMZI based Galois field adder is shown in detail in the Fig. 2.

Here, the fundamental component of this Galois field adder is an all-optical CMZI- based XOR logic gate. The in-depth discussion on the operational principle of CMZI based all-optical XOR logic gate is already provided in our previous paper[28]. Here, we have often used the polarization controllers (PC) to maintain the state of polarization at the outputs of the respective CMZIs.

Now, let us consider the circuit diagram of Fig. 3 to understand the principle of operation of the proposed Galois field adder in the following manner

A 4-bit Galois field adder functions within the context of finite fields, specifically GF(2^n), where n is the number of bits. The addition in Galois fields is accomplished by using the bitwise XOR logic operations, which ensures that the output will remain within the finite field.

Every 4-bit number is regarded as an element of the Galois field GF (2^4). In this finite field, the addition of two elements is performed by XOR operation of their corresponding bits. The field is defined by a primitive polynomial, which ensures the closure property under addition and multiplication.

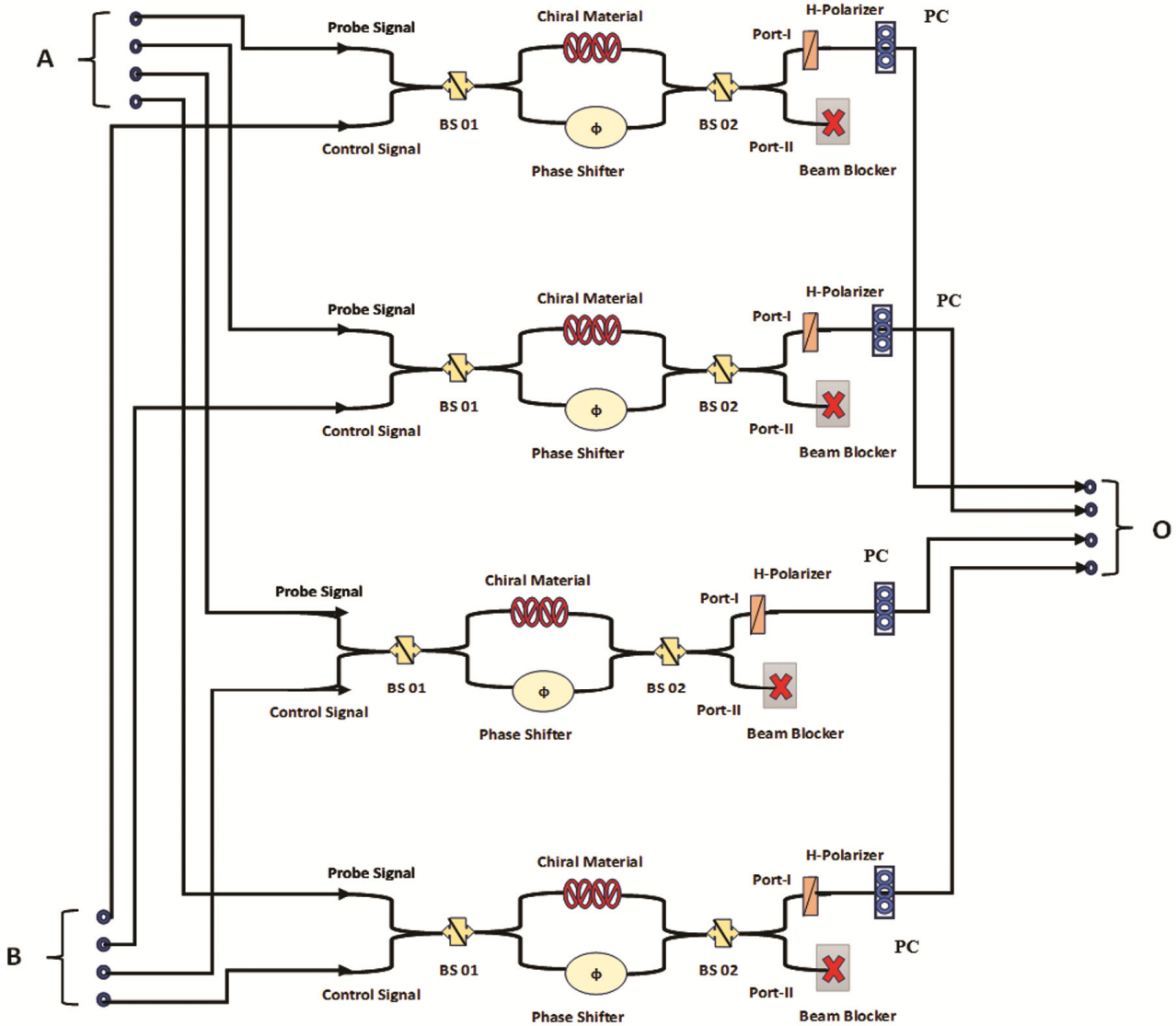

Fig. 2 — Proposed design for CMZI based all-optical GF Adder

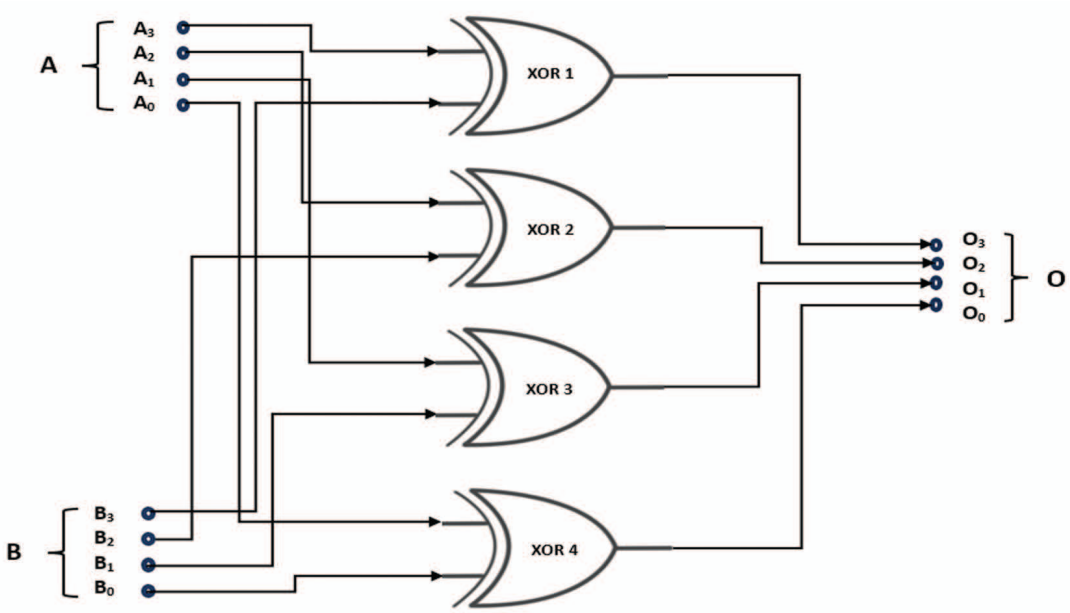

Fig. 3 — Schematic block diagram of CMZI based all-optical Galois field adder (4-bit)

Unlike the conventional binary addition, GF addition is totally carry-free, which provides the faster and more efficient performance in certain all-optical applications.

Therefore, if the augend A and addend B serve as the bit-wise inputs then the proposed all-optical 4-bit GF (2^4) adder essentially performs four parallel XOR operations through four respective CMZI based all-optical XOR gates to obtain the final output O.

The summarized truth table corresponding to a 4-bit Galois field adder is given in Table 2, instead of a single, large truth table.

3 Simulation Results & Discussion

Numerical simulation has been done by using SCILAB simulator to analyse the performance parameters and establish the practical feasibility of the proposed chiral-MZI (CMZI) based all-optical Galois field adder. We have taken the experimental values of the effective transmittances for upper and lower arms i.e., η_1 = 0.98 and η_2 = 0.82[26]. But it is to be noted that both the transmittances correspond to the value of unity in the ideal case. The examples of 4-bit GF addition which are randomly chosen are shown with the corresponding simulated input-output bit-patterns in Figs. 4 (a-d). A summarized truth table is also provided in Table 2, which is relevant to the random examples.

The 4-bit Gaussian pulse trains which have been used as the input signals (augend & addend) are,

Table 2 — Summarized truth table corresponding to a 4-bit Galois field adder

Augend (A)				Addend (B)				Output (O)			
A_3	A_2	A_1	A_0	B_3	B_2	B_1	B_0	O_3	O_2	O_1	O_0
0	1	1	1	1	0	1	0	1	1	0	1
1	0	1	1	0	1	1	0	1	1	0	1
1	0	0	1	0	1	0	0	1	1	0	1
1	0	1	0	0	1	0	1	1	1	1	1

$$A_i = A.\sum_n \exp\left[-\frac{(t-nt_o)^2}{0.7}\right] \quad \ldots (3)$$

where, t_o = 10 ps is the bit repetition rate and 'A' takes the values 0 or 1 depending upon the absence or presence of the optical signal. The output bit-patterns follow the result of Galois field addition in the given four examples as shown in Figs. 4 (a-d). Equation (3) depicts the Gaussian waveforms which show the variation of input/output power (in arbitrary units) with time (in PS). The value of OPD i.e., ΔL = 7.5 mm is taken for simulations which provides 90° rotation in the plane of polarization.

To analyse the all-optical circuit through the different performance parameters such as amplitude modulation ($AM=10\log_{10}\frac{1_{max}}{1_{min}}$), contrast ratio ($CR=10\log_{10}\frac{1_{av}}{0_{av}}$), extinction ratio ($ER=10\log_{10}\frac{1_{min}}{0_{max}}$), quality factor ($Q\text{-factor}=\frac{1_{av}-0_{av}}{\sigma_1+\sigma_0}$) and relative eye-opening [$REO=(1-\frac{0_{max}}{1_{min}})\times 100\%$] are

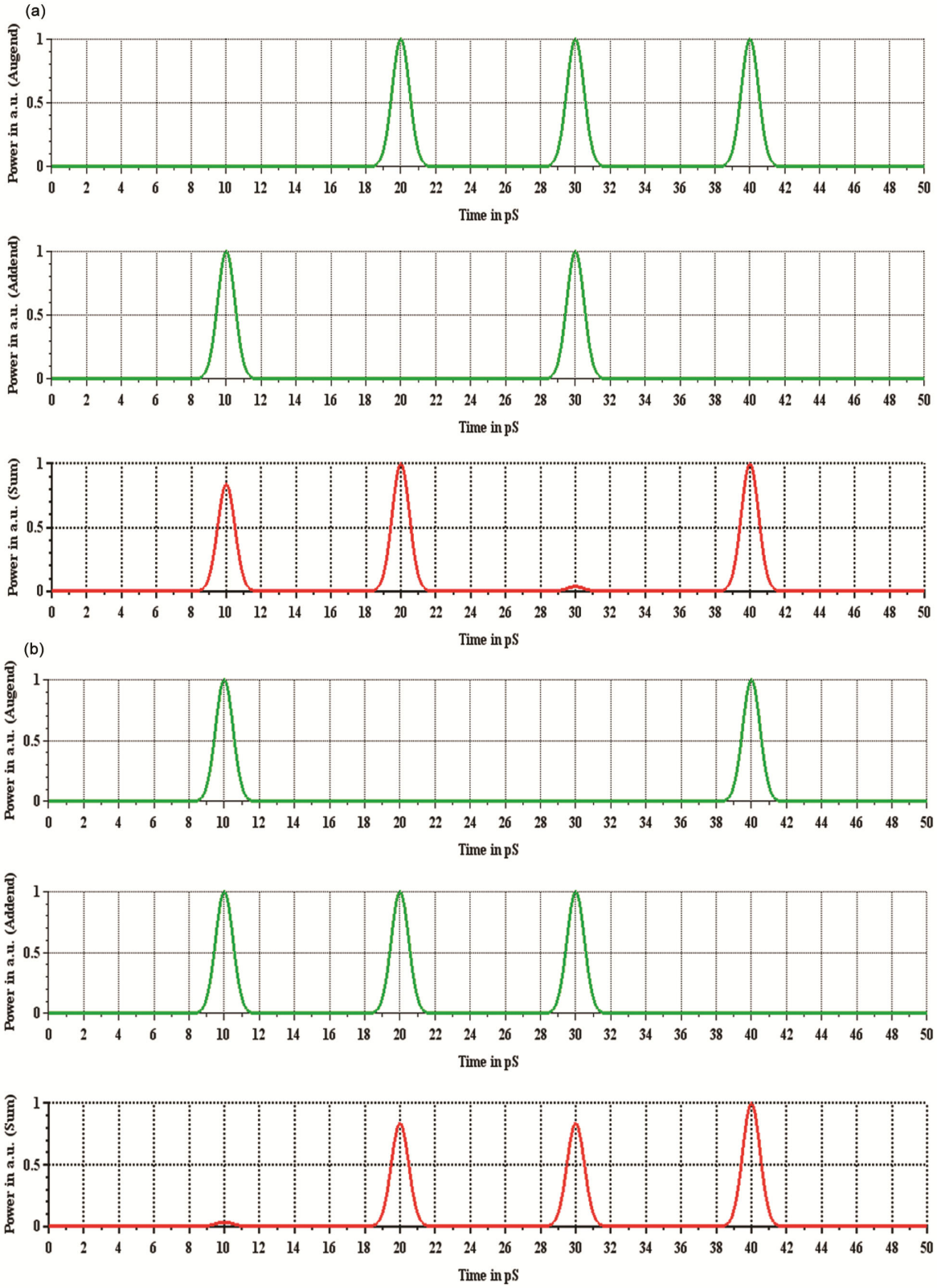

Fig. 4 (a-b) — Arbitrarily chosen examples to understand the all-optical 4-bit Galois field addition operation with the help Gaussian input/output bit patterns

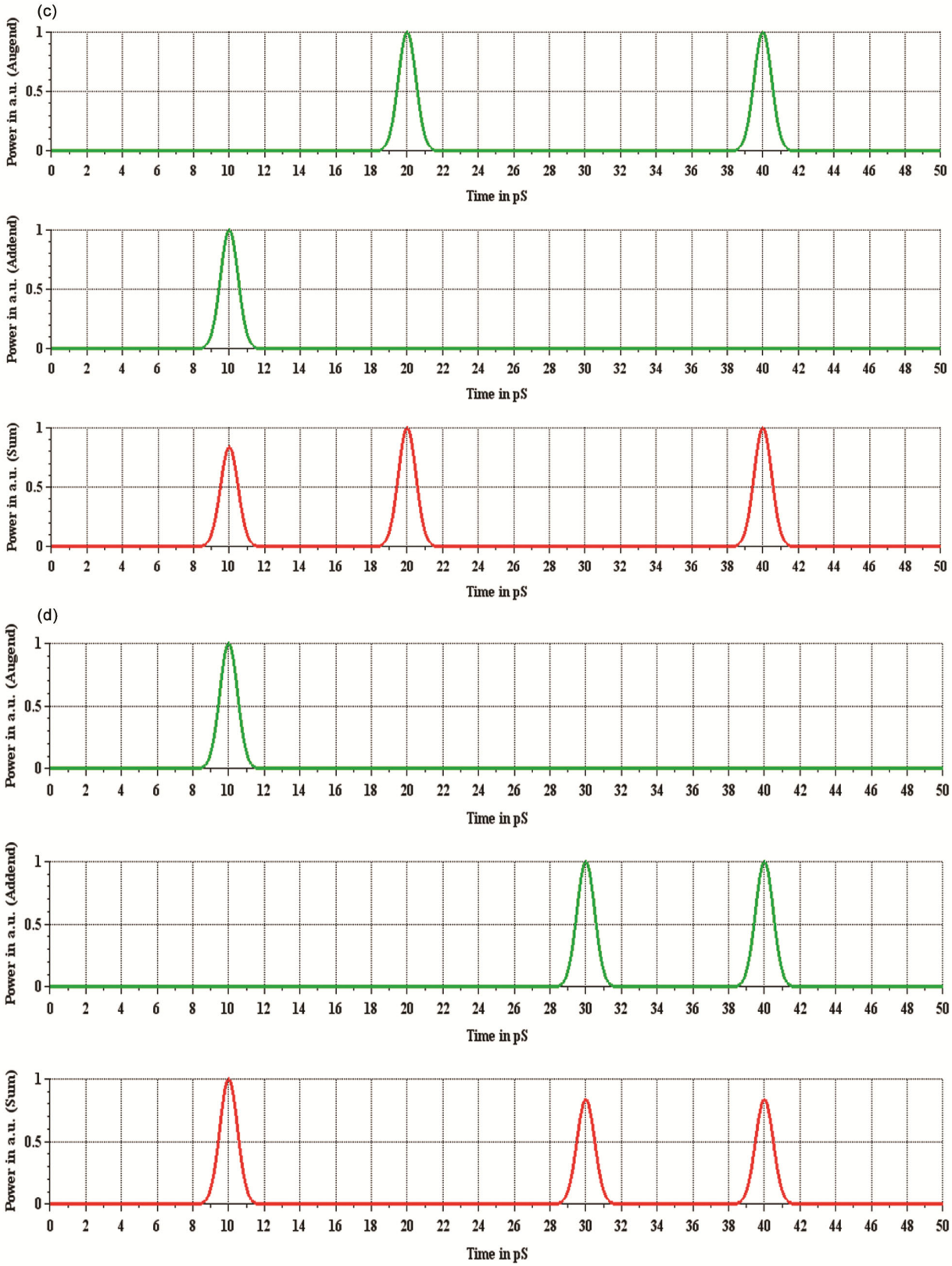

Fig. 4 (c-d) — Arbitrarily chosen examples to understand the all-optical 4-bit Galois field addition operation with the help Gaussian input/output bit patterns

calculated and their variation with transmittance η_1 for η_2=1(ideal case) and η_2=0.82[26] (experimental case) are also investigated which is shown in Figs. 5-9.

Here, the 1_{max},1_{min},1_{av} & σ_1 are the maximum, minimum, average value and standard deviation of the signal bit '1'(LOGIC 1) and the 0_{max},0_{min},0_{av} & σ_0 are the maximum, minimum, average value and standard deviation of the signal bit '0' (LOGIC 0).

To numerically simulate the proposed circuit, the values of different parameters given in the Table 3 as experimentally reported[26] were used.

To analyse numerically, we have taken the value of the signal frequency, ϑ = 384.2793 THz and ΔL = 7.5 mm to achieve 90^0 polarization rotation[26]. Amplitude modulation or AM shows a decrease and then it approaches to an almost saturated value below 0.01dB as expected for efficient practical operation (Fig. 5). This happens when the effective transmittance of lower arm i.e, η_1 tends to the value of η_2 (=1 for ideal case & 0.98 for experimental case[26]. This indicates negligible variations in the high logic levels ('1' state) diminishes and therefore stable outputs. The other performance parameters like the contrast ratio (Fig. 6), extinction ratio (Fig.7), quality factor (Fig. 8) and relative eye-opening (Fig. 9)

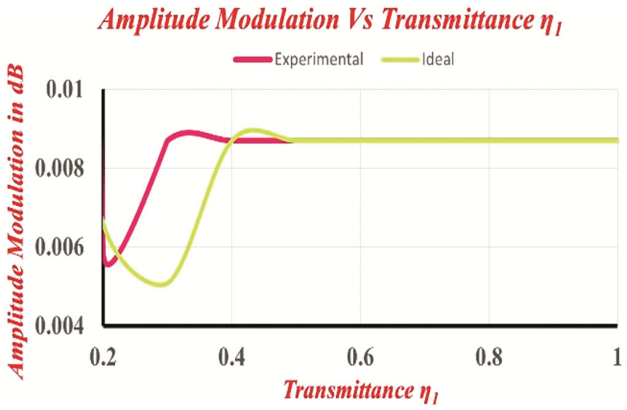

Fig. 5 — The variations of the amplitude modulation with the transmittance η_1 for the given values ofη_2 (Ideal & Experimental Case)

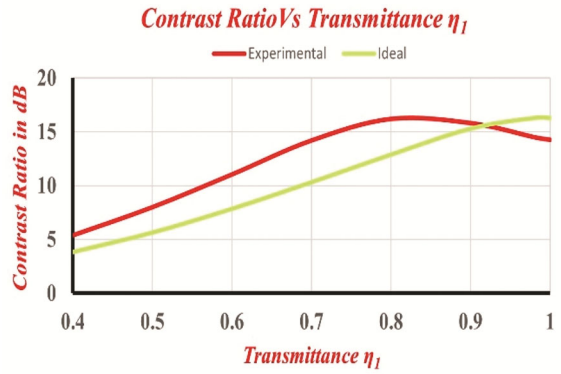

Fig. 6 — The variations of the contrast ratio with the transmittance $\eta_1$for the given values ofη_2 (Ideal & Experimental Case)

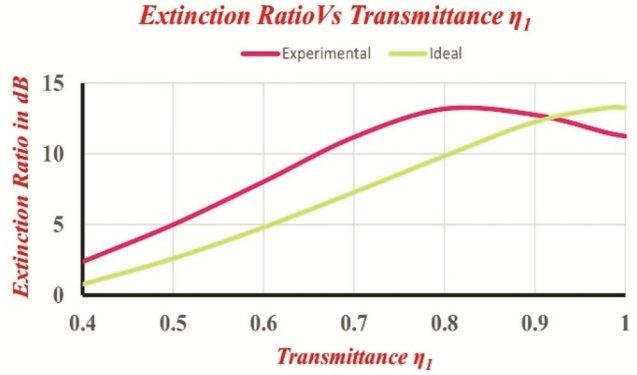

Fig. 7 — The variations of the extinction ratio with the transmittance η_1 for the given values of η_2 (Ideal & Experimental Case)

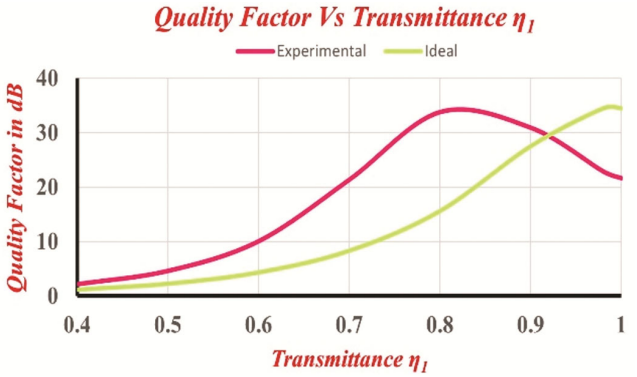

Fig. 8 — The variations of the quality factor with the transmittance η_1 for the given values of η_2 (Ideal & Experimental Case)

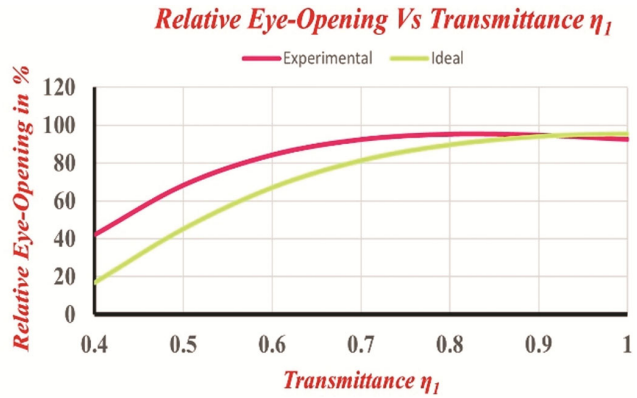

Fig. 9 — The variations of the relative eye-opening with the transmittance η_1 for the given values of η_2 (Ideal & Experimental Case)

Table 3 — Table for parameters used

Parameter	Symbol	Value
Wavelength of the input signals (Same for probe and control signals)	λ	7.80682×10^{-7} m
Frequency of the input signals (Same for probe and control signals)	ϑ	384.2793THz
Effective transmittance at upper arm	η_1	0.98 (Experimental Case) 1 (Ideal Case)
Effective transmittance at lower arm	η_2	0.82 (Experimental Case) 1 (Ideal Case)
Length of the Chiral material (Effective optical path difference)	ΔL	7.5 mm for 90° polarization rotation
Speed of light in vacuum	C	$3 \times 10^8\ m/s$

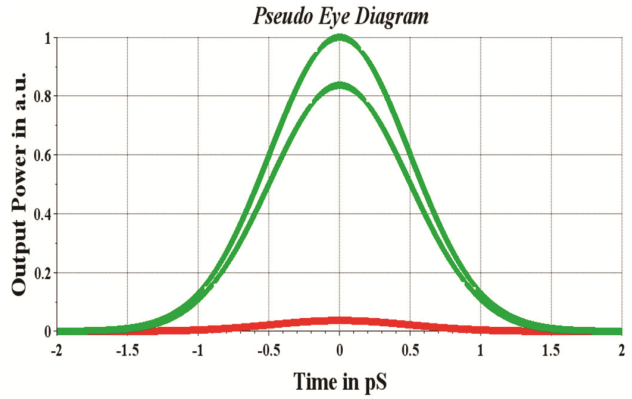

Fig. 10 — Pseudo eye-diagram for 4-bit Galois field adder

Table 4 — Comparison table for performance parameters

Platform	Extinction ratio (in dB)	Contrast ratio (in dB)	Q-factor (in dB)	Relative eye-opening (in %)
2D- Photonic Crystal[35,36]	12.9	8.29	-	-
Graphene-Based Metasurface[37]	-	14.0	-	-
Dual Control Dual SOA TOAD (DCDSTOAD)[38]	-	-	9.82	-
Dual SOA[39]	>50	>55	>50	>94
SOA based MZI[40]	26.01	-	18.74	-
Our proposed work	13.27	16.28	34.48	95.29

increase with η_1. This is also obvious because as the value of η_1 is increased towards η_2, the power of lower logic level decreases and the power of higher logic level increases. The high contrast ratio(16.28 dB) indicates a clear distinction between the lower and higher power levels of the optical signals on an average. Similarly, a high extinction ratio(13.27 dB) ensures a better signal discrimination between low('0') and high('1') states, which helps in error reduction and enhances the clarity of data transmission. Here, the higher value of Q-factor(34.48 dB) is also observed in Fig. 8, which establishes the better signal quality, as it results to a lower probability of bit errors during optical transmission.

In Figs. 9 and 10, the relative eye opening and pseudo eye diagram are shown, which is a powerful tool used in optical and digital communication to investigate the signal integrity and performance. A higher value of relative eye opening (95.29 %) i.e., a larger width and height of the "eye" indicates greater error reduction in distinguishing the higher and lower logic levels, which can also reflect the improved bit error rates (BER). These also ensure higher switching window for transmission and receiving.

From the input-output bit patterns, we get, the insertion loss (IL) = 0.23 dB, which is found to be quite good for ultra-fast operation.

Again, the switching window is also calculated from the pseudo eye-diagram which is equal to 1.0 ps.

The following table compares the values of the performance matrices calculated for our proposed design with other similar works reported earlier[35-40].

Therefore, with the help of Table 4, the CMZI based GF adder reflects quite satisfactory values of the performance parameters in comparison with other previously reported works which establishes the practical feasibility of the proposed design.

3 Conclusion

All-optical chiral Mach Zehnder Interferometer (CMZI) based Galois field adder is proposed and analysed. Higher values of extinction ratio (13.27 dB), contrast ratio (16.28 dB), quality factor (34.48 dB), relative eye-opening (95.29 %) and sufficiently lower value of amplitude modulation (0.008695 dB) has been observed which establish practical feasibility of the Galois field adder. GF adder is widely used in the domain of cryptography, error correction, and digital signal processing etc.

Here, Chiral material-based interferometric switch provides all-optical switching at high speed and at very low power. Thus, this switching module holds significant promise as a transformative component in developing next-generation optical and quantum computational technologies.

References

1 Maji K, Mukherjee K & Mandal M, *Nat Comput*, 24 (2024) 399.
2 Neisy M, Soroosh M & Ansari-Asl K, *Photon Netw Commun*, 35 (2018) 1.
3 Raja A, Mukherjee K & Roy J N, *J Opt*, 51 (2022) 517.
4 Mukherjee K, *J Opt*, 54 (2023) 2072.
5 Mukherjee K & Chattopadhyay T, *Opt Quant Electron*, 54 (2022) 761.
6 Mukherjee K, *J Opt*, 53 (2023) 1501.
7 Yuan M & Sun X, *Proc SPIE*, 6389 (2006) 638919.
8 Li Y, Wu C, Fu S & Dong H, *Proc SPIE*, 5625 (2005) 392.
9 Cherri A K, *Frontiers Optics /Laser Sci XXVII*, OSA Tech Dig Optica Publishing Group, (2011) JWA33.
10 Maji K, Mukherjee K & Mandal M, *Microw Opt Technol Lett*, 66 (2024) e34169.
11 Diebel F, Leykam D, Boguslawski M, Rose P, Denz C & Desyatnikov A, *Appl Phys Lett*, 104 (2014) 261111.
12 Stegeman G I & Wright E M, *Opt Quant Electron*, 22 (1990) 95.
13 Wen Y H, Kuzucu O, Hou T, Lipson M & Gaeta A L, *Opt Lett*, 36 (2011) 1413.
14 Rakshit J K, Selvam P, Kathirvelu S *et al.*, *Braz J Phys*, 55 (2025) 94.
15 Talebzadeh R, Beiranvand R & Moayed S H, *Appl Opt*, 62 (2023) 2936.
16 Liu Q, Ouyang Z, Wu C J, Liu C P & Wang J C, *Opt Express*, 16 (2008) 18992.
17 Rakshit J K, Singh M P, Hossain M *et al.*, *Opt Quant Electron*, 54 (2022) 128.
18 Kibler M R, *Galois Fields and Galois Rings Made Easy* (Elsevier), 2017 p. 33–134.
19 Gyamfi K, Akweittey E & Adusei M, *Int J Sci Res Publ*, 10 (2020) 336.
20 Long G, Sabatini R, Saidaminov M, Lakhwani G, Rasmita A, Liu X, Sargent E & Gao W, *Nat Rev Mater*, 5 (2020) 1.
21 Furlan F, Moreno-Naranjo J M, Gasparini N *et al.*, *Nat Photonics*, 18 (2024) 658.
22 Yi W, Huang H, Lai C, He T, Wang Z, Dai X, Shi Y & Cheng X, *Micromachines*, 15 (2024) 1267.
23 Mehra R, Jaiwal S & Dixit H K, *Proc SPIE*, 8760 (2013) 56.
24 van Vliet S, Alachouzos G, de Vries F K, Pfeifer L & Feringa B L, *Chem Sci*, 13 (2022) 11845.
25 Song G-X, Miao T, Cheng X, Ma H, He Z-X, Zhang W, Zhang Z & Zhu X, *Chin J Polym Sci*, 39 (2021) 1528.
26 Ruan Y, Wu H, Ge S, Tang L, Li Z, Zhang H, Xu F, Hu W, Xiao M, Lu Y & Xia K, *Opt Express*, 30 (2022) 19199.
27 Changder A, Mukherjee K & Roy J N, *Sci Cult*, 90 (2024) 270.
28 Roy J N, Changder A & Mukherjee K, *J Opt*, 54 (2024) 1987.
29 Changder A, Mukherjee K & Roy J, *J Nonlinear Opt Phys Mater*, 34 (2025) 2550001.
30 Rakshit J K, Zoiros K E & Bharti K G, *J Comput Electron*, 20 (2021) 1586.
31 Rakshit J K, Chattopadhyay T, Zoiros K E & Hossain M, *Opt Quant Electron*, 53 (2021) 329.
32 Kotb A, Zoiros K E, Alamer A F & Li W, *Pramana J Phys*, 96 (2022) 396.
33 Zoiros K *et al.*, in *Conf on Optical Fiber Comm*, Tech Dig Ser (2000) pp. 221–223.
34 Zoiros K E & Houbavlis T, *Opt Quant Electron*, 35 (2003) 109.
35 Geerthana S *et al.*, *Laser Phys*, 32 (2022) 106201.
36 Gowri D, Rao S, Swarnakar S, Palacharla V, Seeta K, Raju R & Kumar S, *Photon Netw Commun*, 41 (2021) 109.
37 Meymand R E, Soleymani A & Granpayeh N, *Opt Commun*, 452 (2019) 124772.
38 Maji K, Mukherjee K & Mandal M K, in *Proc IEEE VLSI DCS* (2022) p. 9–12.
39 Raja A, Mukherjee K & Roy J N, *Photon Netw Commun*, 41 (2021) 242.
40 Bosu S & Bhattacharjee B, *J Opt*, 52 (2023) 33.